

) [15].

tails may twist in order to reach areas of lower concentration of some growth-limiting diffusion field. Schultz speculates that this field need not be a concentration of impurities but could also be local stresses generated, for example, by the density difference between solid and liquid. This last suggestion recalls an idea of Tiller and Geering, who used hydrodynamic flows generated by the solid-liquid density difference to account for the splay of spherulites [26,27]. In a recent article, Duan *et al.* give evidence that in very thin polymer films, depletion of the melt in front of the growing film plays a key role in the banding [28].

*Present address: Capilano College, 2055 Purcell Way, N. Vancouver, BC V7J 3H5, Canada.

†Electronic address: johnb@sfu.ca

A number of authors, including Magill [2] and Hutter and Bechhoefer [8], have emphasized that no single theory seems compatible with observations over the full range of systems showing banding (polymers, low-molecular-weight organics, liquid crystals, silicates, etc.) Perhaps different mechanisms are at work in each case, but then why are the macroscopic phenomena so similar?

Faced with these diverging theoretical views on the origins of spherulitic banding, we would like to expand the kinds of experimental measurements available, in order to better constrain the theoretical possibilities. In this article, we explore banded spherulitic growth in a low-molecular-weight material, ethylene carbonate (EC), doped with a small amount of polyacrylonitrile (PAN). To our knowledge, this is the first report of spherulitic growth modes in this system.

knowledge409.6(W)79(emp288.9(sifocus288.9(si)-398.9(sie)-408.9(sienge)sions)2

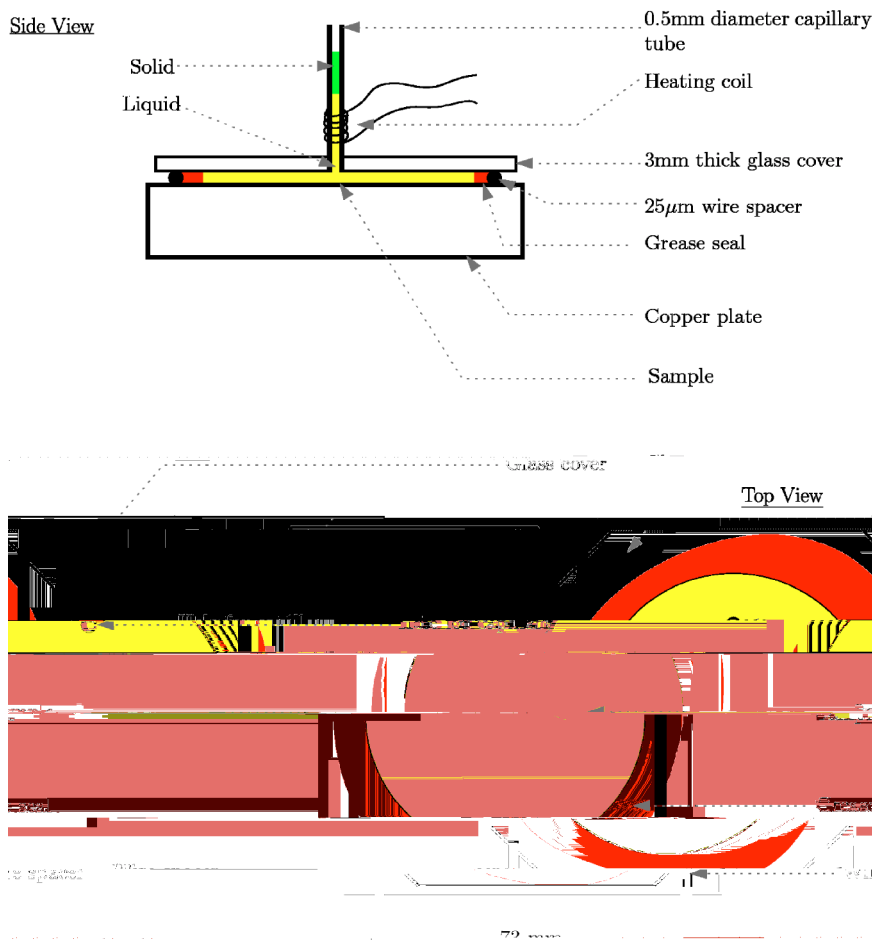


FIG. 1. (Color online). Schematic diagram of sample holder, showing side and top views.

tween to improve thermal contact. The regulator is stable to 1 mK, which far exceeds the experiment's requirements. Temperatures are measured to an accuracy of 0.1 °C by a calibrated thermistor. The sample holder is insulated from the surrounding air by a closed-cell foam box with double-paned glass viewports. The sample was viewed by a CCD camera illuminated off-axis so that specular reflections off the polished, nickel-coated copper plate did not enter the camera's lens.

Preliminary measurements had showed that sample characteristics drift. To assess and reduce drifts, we compared the results of many repeated freezing cycles. This motivated automating the runs. In brief, we created the visual feedback loop mentioned above, monitoring via the CCD camera whether growth had initiated or not. In particular, we could check whether the sample had spontaneously nucleated before reaching the desired undercooling. Without such feedback, it was impossible to obtain the kinds of long, systematic runs needed to track down the sources and magnitudes of the drifts.

The most sensitive monitor of the sample state turned out to be the local front velocity, which is constant but depends on the local temperature and PAN concentration (as well as on impurities resulting from any degradation). To measure the local front velocity, we digitized a movie recording the front growth. Subtracting two successive images removed all but the front, whose intensity profile peak was then fit to a

parabola to extract the front position. We then fit the plot of front position versus time to a low-order polynomial whose derivative is our estimate of the velocity.

Typical results are shown in Fig. 2, which show the effects of multiple runs on sealed and unsealed samples. In a long series of runs, we established that the drifts were not due to segregation of PAN or other impurities produced by the solidification process. We also showed that impurities diffuse in from the sample edge and the area around the nucleation site. In a future version of the experiment, one might improve matters by enclosing the sample in an inert atmosphere. Here, we limited the number of runs so that the drifts and nonuniformity in velocity were less than 2%. In practice, we ensured such stability by retaking the first data point at the end of the run.

B. Undercooling measurements

Because a moving interface releases latent heat, no solidification process can be strictly isothermal. For thin films of polymers ($\sim 1 \mu\text{m}$) frozen at slow growth rates ($\sim \text{nm}/\text{sec}$), the temperature rise at the interface is negligible compared to the undercooling. In our case, faster solidification speeds (mm/sec) and a moderate sample thickness ($25 \mu\text{m}$) imply significant temperature rises (up to 6 °C). Fortunately, for measuring the power law of a critical divergence, knowing that the absolute temperature rise is not necessary. Rather,

one needs only to estimate the differential correction over the range of undercoolings explored ($\Delta T \leq 15$ °C), and even there, only corrections that vary near the divergence undercooling have any effect on the estimate of the critical exponent. While ideally one would measure or calculate the complete temperature field inside the sample, we show by a combination of more simple calculations and experimental measurement that the temperature corrections do not influence our results for the critical exponent.

We begin with the most basic result: Exploring thicknesses ranging from 25 to 75 μm , we observed no change in either the front velocity or band spacing. While this is reassuring, the fact that substantial heating may be expected implies that one should examine this result more closely.

In previous work, we had used an analytical approximation in order to estimate the temperature rise [36]. It is simple to get a rough analytical approximation. The moving front releases a latent heat flux Lv , where L is the molar latent heat and v is the front velocity. The heat must diffuse a distance of the order of the sample thickness d to the copper, which acts as an effective heat sink. The diffusion flux is then roughly $\lambda(\delta T/d)$, where λ is the heat conductivity (nearly the same in both solid and liquid phases) and δT is the typical temperature rise. Equating these fluxes leads to a crude estimate of δT ,

$$\delta T \approx \frac{Lvd}{\lambda} = \frac{Lvd}{D\rho C_p} = a \left(\frac{L}{\rho C_p} \right) \left(\frac{vd}{D} \right). \quad (1)$$

In Eq. (1), $L/\rho C_p = 96.3$ °C is the temperature rise produced by the latent heat in the absence of transport away from the transformed material. The term vd/D is the ‘‘Peclet number’’ N_{pe} , which gives the relative importance of advection and diffusion. We have $v = 1$ mm/s (typically), $d = 25$ μm , and $D_L = 1.00 \times 10^{-7}$ m²/s, giving $N_{\text{pe}} \approx 0.25$ and a nominal temperature rise of 24 °C. The dimensionless constant a was evaluated by numerical simulation using finite-element modeling.

The finite-element modeling of heat flow in our experiment was done using commercial software [

linked to cover all data sets. If a local fit did not show a systematic variation with concentration, we made the parameter a global one. In the end, λ_0 (intrinsic band spacing), A , and α were all fit globally, while the divergence undercooling ΔT_c was fit locally. Figure 5(b) shows a log-log plot of bandspacing against undercooling with the offsets λ_0 and ΔT_c

abrupt transition. One such experimental situation that at least superficially resembles the present one is the divergence of the pitch of a cholesteric liquid crystal in the vicinity of a smectic-A transition. Symmetry requires that the transition be first order, but in practice the discontinuities are very weak. Huang *et al.* measured power-law divergences in several cholesterics, as the temperature was lowered into the smectic phase. The study that is most relevant to our work here is a study of cholesteryl nonanoate doped with a controlled concentration of cholesteryl chloride [45]. In that work, the critical exponent was found to vary with concentration from 0.67 to 1.15. Vigman and Filev have claimed to explain these results as being due to a first-order transition [46,47]. Their theory at least superficially uses many features specific to the free energy of a cholesteric and of a smectic. It would be interesting to revisit their work in a more general context.

Of the three scenarios, the third seems at present most compatible with our results, but more work is required to judge its plausibility. We note that the variation in the cutoff of λ_{max}

shows banded spherulites, and he and Matthew Case did valuable preliminary studies.

APPENDIX: SOME RELEVANT MATERIAL PROPERTIES

Here, we collect some relevant material properties of ethylene carbonate and polyacrylonitrile. Figure 7 shows their

chemical structure, Fig. 8 shows the liquidus line of the EC-PAN phase diagram, and Fig. 9 shows front-velocity measurements as a function of undercooling. These measurements were used to correct the undercooling values. Table I summarizes various thermodynamic properties of EC.

[1] P. J. Phillips, in *Handbook of Crystal Growth*, edited by D. T. J. Hurle (Elsevier, Amsterdam, 1994), Vol. 2, Chap. 18, pp. 1167.

[2] J. H. Magill, *J. Mater. Sci.* **36**, 3143 (2001).

[3]